ACS APPLIED MATERIALS & INTERFACES

www.acsami.org

Research Article

An Inkjet-Printed PEDOT:PSS-Based Stretchable Conductor for Wearable Health Monitoring Device Applications

Li-Wei Lo, Junyi Zhao, Haochuan Wan, Yong Wang, Shantanu Chakrabartty, and Chuan Wang*

Cite This: *ACS Appl. Mater. Interfaces* 2021, 13, 21693–21702

Read Online

ACCESS | Metrics & More | Article Recommendations | Supporting Information

ABSTRACT: A stretchable conductor is one of the key components in soft electronics that allows the seamless integration of electronic devices and sensors on elastic substrates. Its unique advantages of mechanical flexibility and stretchability have enabled a variety of wearable bioelectronic devices that can conformably adapt to curved skin surfaces for long-term health monitoring applications. Here, we report a poly(3,4-ethylenedioxythiophene) polystyrene sulfonate (PEDOT:PSS)-based stretchable polymer blend that can be patterned using an inkjet printing process while exhibiting low sheet resistance and accommodating large mechanical deformations. We have systematically studied the effect of various types of polar solvent additives that can help induce phase separation of PEDOT and PSS grains and change the conformation of a PEDOT chain, thereby improving the electrical property of the film by facilitating charge hopping along the percolating PEDOT network. The optimal ink formulation is achieved by adding 5 wt % ethylene glycol into a pristine PEDOT:PSS aqueous solution, which results in a sheet resistance of as low as 58 Ω/□. Elasticity can also be achieved by blending the above solution with the soft polymer poly(ethylene oxide) (PEO). Thin films of PEDOT:PSS/PEO polymer blends patterned by inkjet printing exhibits a low sheet resistance of 84 Ω/□ and can resist up to 50% tensile strain with minimal changes in electrical performance. With its good conductivity and elasticity, we have further demonstrated the use of the polymer blend as stretchable interconnects and stretchable dry electrodes on a thin polydimethylsiloxane (PDMS) substrate for photoplethysmography (PPG) and electrocardiography (ECG) recording applications. This work shows the potential of using a printed stretchable conducting polymer in low-cost wearable sensor patches for smart health applications.

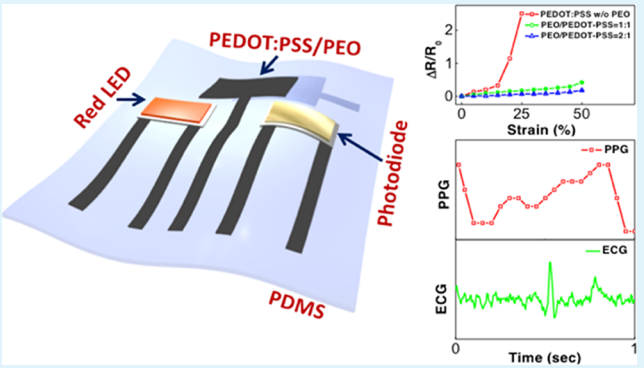

KEYWORDS: *printed electronics, stretchable electronics, conductive polymer, wearable sensors, health monitoring devices*

INTRODUCTION

Over the past decade, flexible electronics such as displays, solar cells, and various types of sensors that can retain their performance and functionality while being bent have been explored extensively.[1−7] Flexible sensors for continuous vital sign monitoring and other health care application have also been developed, but these devices are not ideal because the human skin surface is not only flexible but also soft and stretchable.[8−12] Without being able to form intimate contact and conformably adapt to the human skin, the sensors may detach or slide on the skin, resulting in motion artifact and inaccurate or fluctuating readings. To achieve wearable sensors with more stable signal recording and better wearing comfort, soft electronic devices that are stretchable and have the ability to accommodate large strain and deformations while maintaining their electrical performance have attracted significant attention. Progress has been made in demonstrating soft electronics for applications in artificial electronic skin, soft robotics, and wearable sensors.[13−20]

A stretchable conductor is one of the key components for implementing soft electronics, and there are a few approaches to achieve stretchable conductors. The first is to use conventional metal thin films but pattern them into buckling, wavy, or serpentine-shaped patterns that are structurally stretchable.[21−23] This approach utilizes conventional microfabrication processes that are highly reliable and typically results in great electrical performance, although the sample is sometimes limited to small or medium sizes due to the constraints in microfabrication tools. The second approach is to develop intrinsically stretchable composite materials by adding conductive fillers such as carbon nanotubes (CNT),[24,25] metal nanoparticles, or metal nanowires[26−29]

Received: January 10, 2021
Accepted: March 28, 2021
Published: April 30, 2021

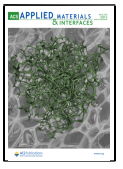

https://doi.org/10.1021/acsami.1c00537
ACS Appl. Mater. Interfaces 2021, 13, 21693−21702

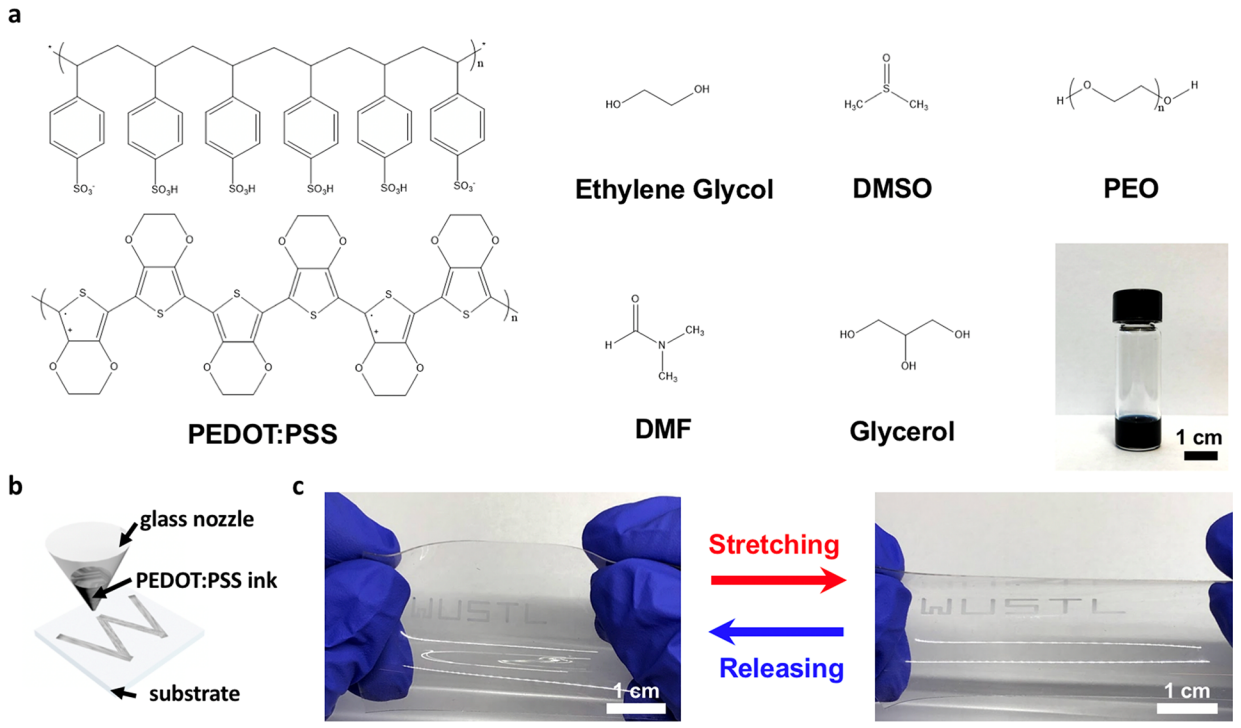

Figure 1. (a) Chemical structures of the conducting polymer PEDOT:PSS; the solvents EG, DMSO, DMF, and glycerol; and the soft polymer PEO and a photo of the optimized ink solution containing the composite of PEDOT:PSS, ethylene glycol, and PEO. (b) Schematic diagram showing the inkjet printing process on the elastomer substrate. (c) Photos showing a PDMS substrate with five layers of printed patterns of the conducting polymer in relaxed and stretched states.

into elastomers such as polydimethylsiloxane (PDMS). Such composite materials generally offer good stretchability, but the use of an insulating polymer matrix could result in either low conductivity or significant conductivity change under mechanical deformation. An alternative method for achieving an intrinsically stretchable polymer is to blend a soft polymer or plasticizer into conducting polymers that may soften the polymer chain and thus increase the free volume, resulting in a low modulus material. For example, it has been reported that the widely used conducting polymer poly(3,4-ethylenedioxythiophene) polystyrene sulfonate (PEDOT:PSS) can be made stretchable by blending in poly(ethylene glycol) (PEG), poly(vinyl alcohol) (PVA), polyurethane (PU), or Zonyl.[30−36] Such polymer blends are solution processable and can be made into large-area conductive thin films for stretchable electrode applications using low-cost processes such as spin coating.[30,33]

To achieve high-resolution patterning of the solution-based stretchable conducting polymer, printing methods such as inkjet printing can be used.[37−41] However, one challenge is that most of the soft polymer additives with high molecular weights are often too viscous. To make the ink suitable for inkjet printing, the viscosity needs to be lowered and its surface tension needs to be adjusted for optimal wetting on elastomer substrates. The above can be achieved by diluting the polymer with appropriate organic solvents.[42,43] In this work, we have systematically studied the effect of adding polar solvents on the most commonly used water-soluble conducting polymer PEDOT:PSS, where PEDOT with positive charges and insulating PSS with negative charges stabilized the PEDOT configuration by columbic attractions.[44] Our study on the electrical properties of PEDOT:PSS mixed with various types of polar solvents have shown that the best conductivity can be achieved by adding ∼5 wt % ethylene glycol (EG).

To achieve stretchability, we have formulated an ink recipe by dissolving the polymer poly(ethylene oxide) (PEO) in *N*,*N*-dimethylformamide (DMF) to reduce its viscosity and then mixing with the PEDOT:PSS solution that can decrease the interaction between polymer chains and increase the free volume between PEDOT and PSS grains to make a highly stretchable ink with low sheet resistance.[16] After being patterned using inkjet printing, thin films of an intrinsically stretchable PEDOT:PSS/PEO polymer blend exhibit a low sheet resistance of 84 Ω/□ and a high stretchability of up to 50%. In addition to its high stretchability and conductivity, the PEDOT:PSS/PEO polymer blend is also biocompatible and can be made into wearable sensor patches for health monitoring applications.[45−48] As an example, we have demonstrated an inkjet-printed sensor patch on a PDMS substrate for recording vital signs including electrocardiography (ECG) and photoplethysmography (PPG). Unlike traditional Ag/AgCl electrodes with a conducting hydrogel between the skin and electrodes, the printed PEDOT:PSS/PEO polymer blend not only is stretchable but also can be used as dry electrodes that can be directly placed on the skin surface without the use of a conducting hydrogel. In the PPG monitoring application, the printed PEDOT:PSS/PEO is used as stretchable interconnects for connecting a surface-mounted light-emitting diode and a photodetector. The printed sensor patch can simultaneously and continuously record ECG and PPG waveforms for monitoring the heart rate, blood oxygen, and cardiac cycles. It serves as a proof-of-concept demonstration to show the potential of using a printed stretchable conducting polymer in low-cost wearable sensor patches for smart health applications.

https://doi.org/10.1021/acsami.1c00537
ACS Appl. Mater. Interfaces 2021, 13, 21693−21702

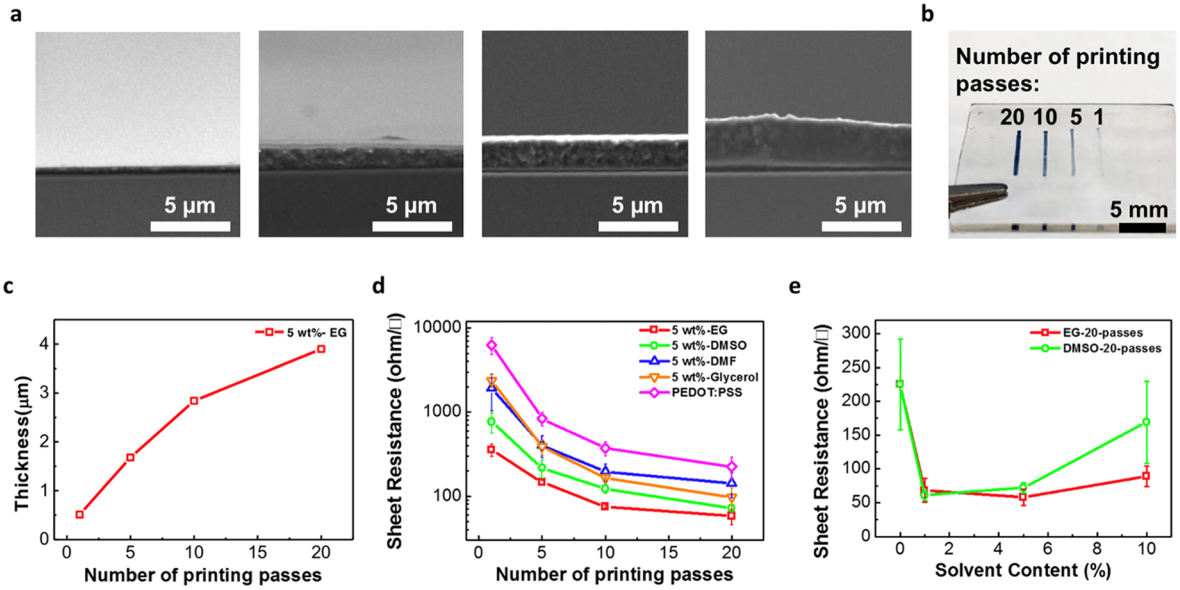

Figure 2. (a) SEM images showing the thickness of the inkjet-printed PEDOT:PSS thin film with 5 wt % EG after 1, 5, 10, and 20 print passes (from left to right), respectively. (b) Photograph of the inkjet-printed PEDOT:PSS thin film on PDMS with various numbers of print passes. (c) Thickness of the inkjet-printed PEDOT:PSS thin film with 5 wt % EG vs the number of print passes. (d) Comparison of the sheet resistance between the pristine PEDOT:PSS ink and PEDOT:PSS mixed with 5 wt % of various types of polar solvent additives after various numbers of print passes. (e) Comparison between the sheet resistance of the PEDOT:PSS thin film with EG or DMSO additives with various amounts of polar solvent content from 0, 1, and 5% to 10%.

RESULTS AND DISCUSSION

The chemical structures of the conducting polymer PEDOT:PSS; the polar solvents EG, dimethyl sulfoxide (DMSO), DMF, and glycerol; and the soft PEO are shown in Figure 1a. PEDOT is the most widely used conducting polymer in the past decade due to its high conductivity, transparency, and stability. The most commonly used commercially available product of PEDOT comes with PEDOT doped with PSS. This aqueous dispersion consisting of PEDOT-rich particles is surrounded by PSS-rich shells, with the negatively charged polyanion (PSS^-) stabilizing the positively charged polycation ($PEDOT^+$). The polyanion (PSS^-) is an insulator that hampers the charge transport pathway through polycation ($PEDOT^+$) and results in a low electrical conductivity of less than 1 S cm^{-1} in pristine PEDOT:PSS. One of the solutions to improve its conductivity is by adding polar solvents into the pristine PEDOT:PSS aqueous solution to achieve phase separation between PEDOT and PSS grains and the conformational change of the PEDOT chain.[49,50] The detailed mechanism and experimental results will be discussed later. Despite the increase of conductivity after the addition of a polar solvent, the mechanical properties of the PEDOT:PSS thin film are too brittle to resist any large deformations. To address the challenge, here we report a method for achieving a printable and stretchable conducting polymer by blending a soft polymer poly(ethylene oxide) (PEO) and EG solvent with PEDOT:PSS. The rearranged microstructure of rigid PEDOT grains and soft PSS/PEO domains would remove the brittleness of PEDOT:PSS and yield a stretchable PEDOT:PSS/PEO polymer blend. As schematically illustrated in Figure 1b, such polymer ink can be formulated to the appropriate viscosity to allow it to be directly patterned using the inkjet printing process. To facilitate the wetting of the ink on hydrophobic surfaces such as PDMS, the elastomeric substrate can be pretreated with oxygen plasma. After treatment, the PEDOT:PSS/PEO composite ink can be patterned onto the pretreated PDMS substrate with a feature size as small as 400 μm. More details about the ink formulation and printing process can be found in the experimental section. Figure 1c shows a sample with the composite PEDOT:PSS/PEO ink printed on a 0.5 mm thick PDMS substrate. The composite polymer thin film exhibits high stretchability without any crack formation after multiple stretching cycles with tensile strain up to 50%.

While the polar solvent additives can address the low conductivity of pristine PEDOT:PSS, the number of printing passes and consequently the film thickness also play an important role in both the optical and electrical properties of the printed PEDOT:PSS thin film. As shown in Figure 2, we have systematically studied the effect of printing passes on the film thickness and the sheet resistance of the printed thin films with various types of solvent additives. The cross-sectional scanning electron microscope (SEM) images taken from the inkjet-printed PEDOT:PSS thin films with 5 wt % EG are shown in Figure 2a. With 1, 5, 10, and 20 printing processes, the printed PEDOT:PSS film thickness increases monotonically, which also causes the transparency of the PEDOT:PSS thin film to decrease as shown in Figure 2b. The relationship between the film thickness with respect to the printing passes is presented in Figure 2c. The thicknesses of 1, 5, 10, and 20 printing passes are measured to be 0.51, 1.68, 2.84, and 3.9 μm, respectively. The corresponding UV−vis spectra of the inkjet-printed PEDOT:PSS thin film is presented in Supporting Information Figure S1.

To determine the best polar solvent additive, we have systematically studied the electrical properties of printed PEDOT:PSS thin films with EG, DMSO, DMF, and glycerol. An amount of 5 wt % of each polar solvent was mixed into a separate surfactant-free PEDOT:PSS aqueous solution (1.1% in H_2O, surfactant-free, high-conductivity grade). Additionally, 1 wt % Triton-X was also added into the solution to tune its

https://doi.org/10.1021/acsami.1c00537
ACS Appl. Mater. Interfaces 2021, 13, 21693−21702

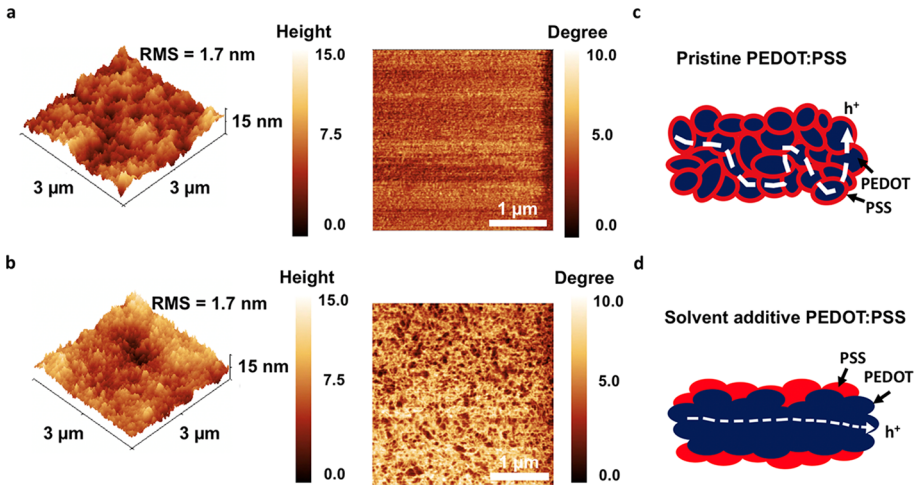

Figure 3. Morphology of the pristine PEDOT:PSS and PEDOT:PSS thin films with 5 wt % EG. Height and phase images of printed thin films of (a) PEDOT:PSS and (b) PEDOT:PSS with 5 wt % EG obtained with tapping-mode AFM. (c) Schematic illustration of the hole transport in the pristine PEDOT:PSS thin film. (d) Schematic illustrating the PEDOT:PSS phase separation and structural rearrangement after the addition of EG.

surface energy for optimal inkjet printing results. After printing, the film was placed on a hot plate and annealed at 120 °C for 15 min. The comparison of sheet resistance for various solvent additives with different numbers of printing passes is shown in Figure 2d. As expected, the data from the solvent-free PEDOT:PSS aqueous ink exhibit the highest sheet resistance of ∼6.2 kΩ/□ with a single pass printing. Other films with polar solvent additives show significantly lower sheet resistance, with 5 wt % EG exhibiting the lowest sheet resistance of ∼355 Ω/□. The samples with 5 wt % DMSO, 5 wt % DMF, and 5 wt % glycerol exhibit sheet resistance values of 767, 1914, and 2371 Ω/□, respectively. The results above indicate that polar solvents are indeed effective in improving the electrical property of the PEDOT:PSS. To reach an even lower sheet resistance, the number of printing passes can be increased. With 20 passes, the sample with 5 wt % EG additive exhibits the lowest sheet resistance of 58 Ω/□ and the one with 5 wt % DMSO exhibits the second lowest sheet resistance of 72 Ω/□. Furthermore, according to Figure 2d, both EG and DMSO additives are effective in lowering the sheet resistance of PEDOT:PSS. To have a better understanding of both additives and find the optimal ink composition, we have also compared the sheet resistance of PEDOT:PSS inks with different amounts of solvent additives ranging from 0 to 10 wt % as shown in Figure 2e. The results show that the PEDOT:PSS thin films with 1 wt % DMSO exhibit a slightly lower sheet resistance of 61 Ω/□ compared to 68 Ω/□ from the sample with 1 wt % EG. As the solvent content increases to 10 wt %, samples with both types of additives show inferior performance compared to 1 and 5 wt %. The optimal ink formulations for DMSO and EG were obtained at 1 and 5 wt %, respectively. However, because the one with 5 wt % EG exhibits the lowest sheet resistance among all experimental conditions, we have chosen this as the optimal ink formulation for further experiments.

The decrease in sheet resistance in the printed PEDOT:PSS thin film with the EG additive can be attributed to the morphology change of the PEDOT and PSS grains. High-resolution topography and phase images of the surface of the printed PEDOT:PSS thin films obtained using atomic force microscopy (AFM) are shown in Figure 3a,b. It has been reported that PEDOT and PSS grains can be differentiated by using AFM phase images,[51] where the dark regions correspond to soft materials and the bright regions correspond to more rigid polymers. In the PEDOT:PSS thin film, PSS is considered as a softer polymer and PEDOT is considered to be more rigid.[35] Figure 3a shows the height image of the pristine PEDOT:PSS thin film with a root-mean-square roughness of 1.7 nm, and the phase image indicates that small PEDOT grains are surrounded by small PSS grains. These insulating PSS grains hinder the carrier transport and impede the charge hopping with a discontinuous conducting pathway of PEDOT that results in a less conductive film. With the addition of EG, the PEDOT and PSS grains rearrange with thermal annealing, which separates the PEDOT grains from PSS grains as shown in Figure 3b. The microstructure of the thin film is more percolated due to the aggregation of the PEDOT grains (the brighter region in the phase image), and this percolating network could aid the charge hopping along the chain that leads to a more conductive film. The effect of the aforementioned morphology change with the help of a polar solvent is schematically illustrated in Figure 3c,d.

Although the thin film of PEDOT:PSS with the EG additive exhibits superior sheet resistance, the film is still unable to resist any significant deformation. When a large tensile strain (greater than 25%) is applied, the sheet resistance of the film will increase over 250% due to the formation and propagation of microcracks. To make the conducting polymer stretchable, one possible way is to add soft polymer blends or plasticizers to decrease the interaction between polymer chains and increase the free volume between PEDOT and PSS grains.[52] Previous literature has shown that adding a soft polymer such as PEG, PVA, PDMS, or PU into PEDOT:PSS to form polymer blends can effectively decrease the Young's modulus and increase the elongation at break (Supporting Information Table S1).[30,31,33,53,54] While this approach could result in the desired elasticity, the PEDOT:PSS polymer blends may also experience a decrease in electrical conductivity due to the insulation of these soft polymers. Moreover, some soft polymers such as PDMS are intrinsically hydrophobic and may be difficult to mix uniformly in the aqueous PEDOT:PSS solution, and its high viscosity also makes it challenging to fabricate high-resolution patterns through inkjet printing. In this work, we have selected the water-soluble soft polymer

https://doi.org/10.1021/acsami.1c00537
ACS Appl. Mater. Interfaces 2021, 13, 21693−21702

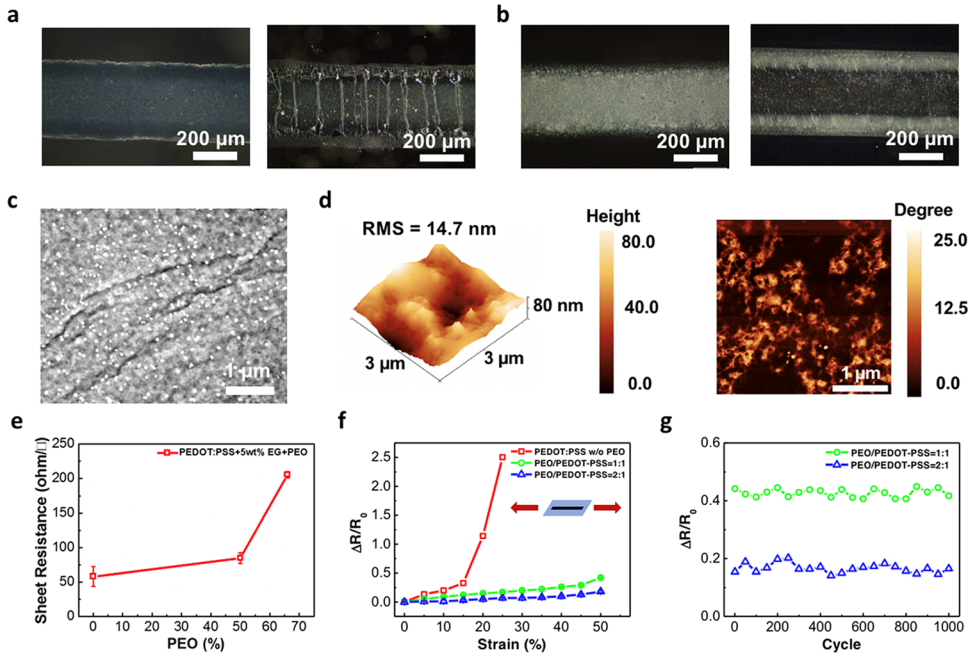

Figure 4. (a) Optical micrographs of printed thin films of PEDOT:PSS with 5 wt % EG under 0% (left) and 50% (right) of tensile strain showing the propagation of microcracks and structural failure when the film is stretched. (b) Optical micrographs of printed thin films of PEDOT:PSS with 5 wt % EG and 66 wt % PEO under 0% (left) and 50% (right) of tensile strain indicating that significantly fewer cracks appear in the thin film. (c) SEM image showing the microstructure of the PEDOT:PSS thin film with 5 wt % EG and 66 wt % PEO. (d) Tapping-mode AFM height and phase images showing the surface morphology of the PEDOT:PSS thin film with 5 wt % EG and 66 wt % PEO. (e) Sheet resistance of the inkjet-printed PEDOT:PSS thin film with 5 wt % EG and various amounts of PEO. (f) Relative change in resistance plotted as a function of tensile strain for the PEDOT:PSS thin film with 5 wt % EG and various amounts of PEO. (g) Electrical property of the PEDOT:PSS/PEO film under the cyclic stretching test with 50% tensile strain.

PEO as the polymer filler that can effectively encompass the brittle PEDOT and soft PSS grains.[55] In addition to making the PEDOT:PSS film stretchable, PEO can also facilitate the phase separation of PEDOT and PSS grains to form a more conductive network of PEDOT grains, which can offset the decrease in electrical conductivity due to the addition of insulating fillers. Unlike the solvent additives described above, PEO remains in the printed PEDOT:PSS thin film even after annealing at elevated temperatures. The hydroxyl groups on PEO may form strong hydrogen bonds with the sulfonic groups on PSS, thereby weakening the interaction between PEDOT and PSS chain and thus forming a more connective PEDOT network.[56] As a result, adding PEO into PEDOT:PSS and EG can result in highly stretchable thin films while maintaining its electrical performance.

We have compared the structure change of thin films of PEDOT:PSS with the EG additive before and after adding PEO. The thin films were inkjet-printed onto the PDMS substrate followed by thermal annealing at 120 °C for 15 min, and the samples were then mounted on a linear stage for the stretch test. Figure 4a shows the optical micrographs of printed thin films of PEDOT:PSS with 5 wt % EG in its relaxed state (left) and when being stretched to 50% (right). Under 50% tensile strain, the formation of microcracks can be easily seen from the images, which greatly affects the electrical properties of the film. In contrast, according to Figure 4b, similar printed thin films of PEDOT:PSS with 5 wt % EG and 66 wt % PEO additives show only minor cracks at the edges of the pattern under the same amount of strain. The SEM image of the PEDOT:PSS thin film with 5 wt % EG and 66 wt % PEO is presented in Figure 4c. The image shows the incorporation of crystalline PEO within the PEDOT:PSS thin film. Moreover, AFM images in Figure 4d show larger bright regions compared with the phase image in Figure 3b, which indicate that the PEDOT grains and the dark regions are soft PEO and PSS. The incorporation of PEO in PEDOT forms a percolation network as expected, which aids the charge transport similar to the effect of polar solvents. However, the decrease in the PEDOT concentration and increase in the PEO content can also negatively affect the electrical property of the PEDOT:PSS/PEO polymer blend. Figure 4e shows the sheet resistance of the film with various amounts of PEO. Before adding PEO, the sheet resistance of the PEDOT:PSS thin film with 5 wt % EG is ~58 Ω/□. With 50 wt % (1:1) or 66 wt % (1:2) of PEO added, the sheet resistance values increase to ~84 and 205 Ω/□, respectively. More details of the stability of the inkjet-printed PEDOT:PSS thin film over time is presented in Supporting Information Figure S2. The results are expected due to the lower percentage of PEDOT presented in the solution and the presence of insulated PEO.

Besides the effect of the PEO additive on sheet resistance, the change in the electromechanical property is also examined through stretch tests and the results are presented in Figure 4f. PDMS substrates (0.5 mm thick) with printed PEDOT:PSS or PEDOT:PSS/PEO thin films were mounted on a linear stage, and liquid metal (EGaIn) droplets were placed on both ends of the films for measurement purposes. The electrical measurements were performed after the fresh samples were first stretched for 20 cycles. The PEDOT:PSS sample without PEO exhibits a poor mechanical property with the sheet resistance increasing by 20% ($\Delta R/R_0$ = 0.2, where ΔR is the change in sheet resistance and R_0 is the sheet resistance in the relaxed

https://doi.org/10.1021/acsami.1c00537
ACS Appl. Mater. Interfaces 2021, 13, 21693−21702

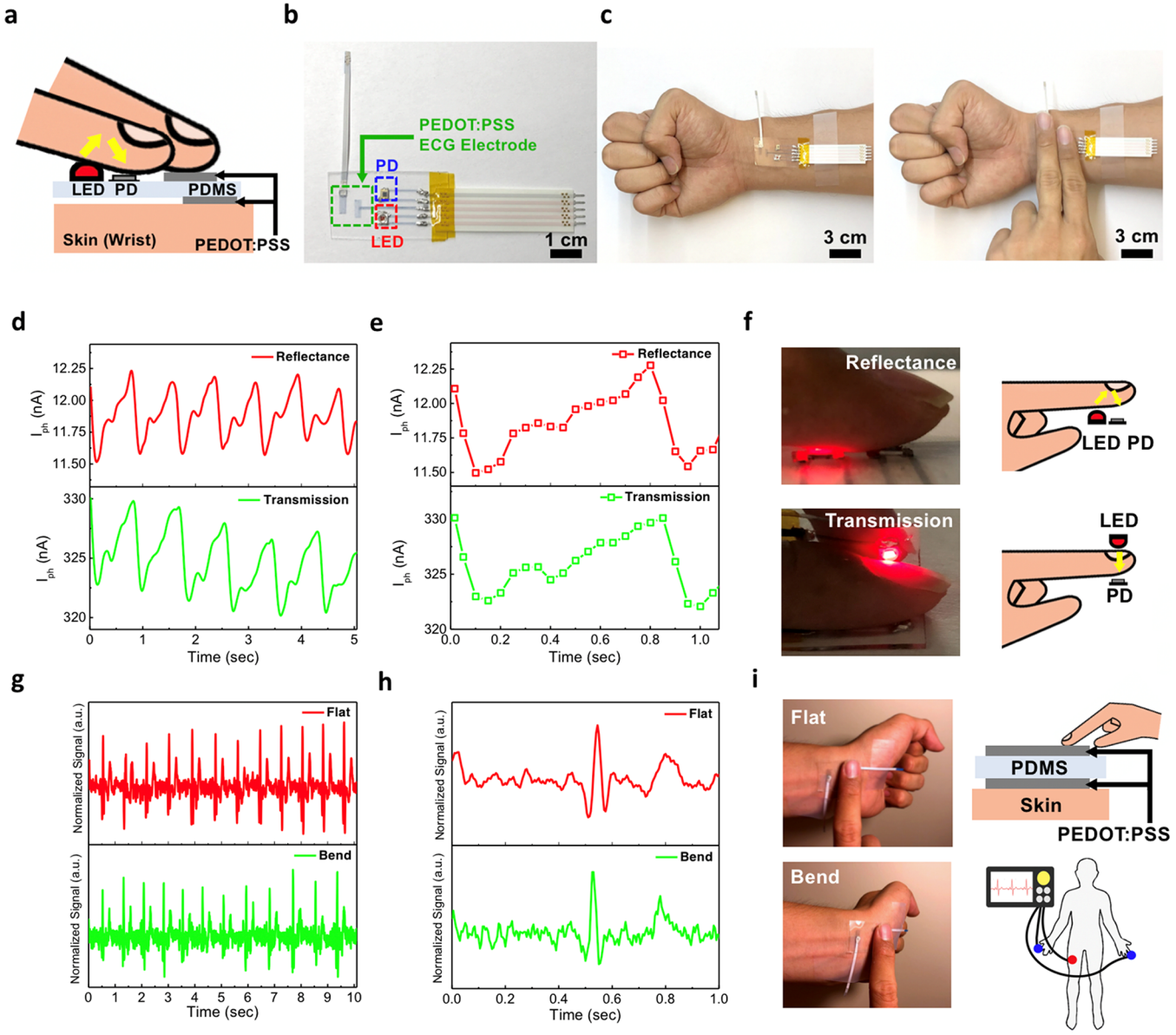

Figure 5. Representative applications of the printed stretchable PEDOT:PSS/PEO conductor for wearable electrocardiography (ECG) and photoplethysmography (PPG) sensors. (a) Schematic diagram of a PDMS patch with integrated ECG and PPG sensors for simultaneous recording of both physiological signals. (b) Photograph of the sensor patch with integrated ECG and PPG sensors. (c) Photograph showing the placement of the sensor patch on a human body for ECG and PPG recording. (d, e) PPG waveforms measured with 625 nm LED illumination using both reflective and transmission modes. (f) Photographs showing the experimental setup for reflectance and transmission mode PPG measurement. (g, h) ECG signals measured with printed PEDOT:PSS/EG/PEO electrodes. (i) Photographs and schematics showing the ECG electrode placement on the skin surface during the ECG measurements.

state) when the film is stretched by 10%. Moreover, the sheet resistance increases dramatically by 250% ($\Delta R/R_0$ = 2.5) under 25% tensile strain. In contrast, for the samples with 50 or 66 wt % PEO additives, under 10% tensile strain, the sheet resistance increases by only 9 or 1%, respectively. As the tensile strain increases to 50%, the sample with 50 wt % PEO additive experienced a 41% increase in sheet resistance, while the one with 66 wt % PEO additives only rose by 18%. We have also studied the electrical properties of the PEDOT:PSS/PEO thin film when stretched in the transverse direction, and the data are presented in Supporting Information Figure S3. The results clearly show that the PEO additive is very effective in rendering the PEDOT:PSS film stretchable. The stability of the PEDOT:PSS/PEO polymer blend under cyclic stretch tests was also studied, and the results are presented in Figure 4g. The samples with the PEDOT:PSS/PEO polymer blend were repeatedly stretched to 50% tensile strain for 1000 cycles, and $\Delta R/R_0$ remained almost unchanged at 42 or 20% for the samples with 50 or 66 wt % PEO, respectively.

In both ink formulations, the PEDOT:PSS/PEO polymer blends show good stability and compliance to mechanical strain without significant sacrifice in electrical performance. Although the ink with 66% of PEO offers the best stretchability, the sheet resistance is also much higher compared to the one with 50% of PEO. For wearable electronics applications, the human skin surface normally experiences no more than 30% tensile strain.[57] As a result, it is

https://doi.org/10.1021/acsami.1c00537
ACS Appl. Mater. Interfaces 2021, 13, 21693−21702

a good tradeoff to choose the formulation with 50 wt % PEO additive.

The above PEDOT:PSS/PEO composite ink can be processed into intrinsically stretchable electrodes or conductors for wearable electronics and bioelectronic applications. In Figure 5, we have demonstrated an inkjet-printed PEDOT:PSS-based soft sensor patch for electrocardiography (ECG) and photoplethysmography (PPG) recording, allowing users to track the cardiac activity, cardiac cycle, and heart rate simultaneously. The schematic and photograph of the prototype of the integrated soft sensor patch are shown in Figure 5a,b. As an exemplary use case, the user may attach the sensor patch on his or her right wrist where one of the printed PEDOT:PSS/PEO electrodes on the backside of the PDMS substrate is in close contact with the skin. One finger from the left hand can then be placed on top of another ECG electrode on the front side of the PDMS substrate, and the other finger can be placed on the PPG sensor comprising a red light-emitting diode (LED) and a photodiode (PD) (Figure 5c). Demonstration of the PPG recording is represented in Figure 5d–f, where the printed PEDOT:PSS/PEO film serves as stretchable interconnects between rigid circuit components (surface-mounted LED and PD). The PPG sensor can be used in both reflectance and transmission modes (Figure 5f). In the reflectance mode, the red LED and PD are placed on the same side of the finger. Due to the fact that blood absorbs more light than surrounding tissues, the small variations in the volume change between systolic and diastolic phases can be observed by the intensity change of backscattered light reaching to the photodiode.[58] In addition to the reflectance mode, the soft sensor patch can also be wrapped around the fingertip and transformed into a transmission mode PPG. The red LED is now located at the fingernail, whereas the PD is placed at the bottom of the fingertip. The photodiode then detects the intensity of the transmitted light through the tissue and blood vessel. Both modes of the PPG recordings provided valuable signals of the heart rate and cardiovascular system activity. Both modes of PPG waveforms were recorded and are presented in Figure 5d,e. The waveforms show clear periodic peaks that correspond to a heart rate of 72 bpm.

The printed stretchable PEDOT:PSS/PEO polymer blend can also be used as a dry electrode for ECG recording applications, and the results are presented in Figure 5g–i. The PEDOT:PSS/PEO electrodes were inkjet-printed on both sides of the PDMS substrate with one electrode attached on the user's wrist and another attached to the finger, while a third electrode is placed on the user's thigh and served as a ground electrode. The three electrodes were connected to a commercial ECG monitor IC (AD8232, SparkFun) for data recording. To illustrate that the soft sensor patch can conformably adapt to the skin and the stretchability of the electrodes, two sets of ECG measurements were performed with the wrist flat and bent. Both waveforms in Figure 5g are periodic and represent the phases of electrical activity of the heartbeat. The two waveforms closely resemble each other, which demonstrate the stretchability of the PEDOT:PSS electrodes without mechanical or electrical failure under applied strain in a bent wrist. In Figure 5h, the recorded ECG waveforms exhibit clearly distinguishable QRS interval and T waves in which the QRS complex represents ventricular depolarization and the T waves reflect the ventricular repolarization.[59] These signals can be further used to detect cardiovascular diseases, such as arrhythmias and myocardial infarction.[60,61]

CONCLUSIONS

In summary, we have developed an inkjet-printable and stretchable PEDOT:PSS/PEO polymer blend with PEO to help improve elasticity and a polar solvent to help improve electrical conductivity and tune the ink rheology. Using the optimal ink formulation and printing recipe, printed thin films with a low sheet resistance of 84 Ω/□ that can resist up to 50% tensile strain for thousands of cycles have been achieved. We have further demonstrated that the stretchable polymer blends can be used as printed interconnects and electrodes to form an ultrathin wearable sensor patch for PPG and ECG monitoring applications. In particular, PPG was demonstrated in both reflectance and transmission mode, and the recorded signal clearly shows the pulsatile nature of blood in the tissue with indication of periodic systolic and diastolic peaks. The ECG waveforms collected from the polymer electrodes represent the activity of the ventricle during different phases of heartbeats. The highly elastic conductive material and lightweight soft sensor patch developed in this work may lead to low-cost wearables for vital sign and cardiovascular disease monitoring and various other smart connected health applications.

METHODS

Materials. Poly(3,4-ethylenedioxythiophene)−poly-(styrenesulfonate) (1.1% in H_2O, surfactant-free, high-conductivity grade), ethylene glycol (EG) (anhydrous, 99.8%), dimethyl sulfoxide (DMSO) (anhydrous, ≥99.9%), *N*,*N*-dimethylformamide (DMF) (anhydrous, 99.8%), glycerol (99.5%), poly(ethylene oxide) (PEO) (powder, average $M_v \sim$ 5,000,000), and Triton-X 100 (laboratory grade) were purchased from Sigma-Aldrich. Eutectic gallium−indium (EGaIn) was purchased from RotoMetals, and the silver conductive epoxy was purchased from MG Chemicals. Polydimethylsiloxane (PDMS) (Sylgard 184) was purchased from Dow Corning.

Preparation of the PEDOT:PSS/PEO Ink Solution. Polar solvents (EG, DMSO, DMF, and glycerol) from 1, 5, or 10 wt % incorporated with 1 wt % Triton-X 100 as surfactant were added into a surfactant-free PEDOT:PSS aqueous solution. The prepared solution was then stirred at room temperature for 2 h. PEO was first dissolved in DMF to give a concentration of 10 mg/mL. Afterward, 5 wt % ethylene glycol, 1 wt % Triton-X 100, and the desired weight ratio of the PEO solution were then added into the surfactant-free PEDOT:PSS aqueous solution. The solution was then stirred at room temperature for 3 h. The weight fraction of each solvent or additive was calculated from the additive weight divided by the total weight of the solution.

Preparation of the PDMS Substrate. The PDMS substrate was prepared by mixing the PDMS prepolymer with the curing agent with a mixing ratio of 10:1 w/w. Two Rain-X (ITW Global Brands) pretreated glass slides with a dimension of 1.5 × 1 in and a 0.5 mm spacer were then used to cast a 0.5 mm thick PDMS substrate. A vacuum desiccator was used to eliminate the bubbles from the film, and the sample was subsequently cured at 80 °C for 3 h.

Inkjet Printing of the PEDOT:PSS Thin Film on PDMS. The PDMS substrate was pretreated by oxygen plasma at 30 W for 15 s. The as-prepared PEDOT:PSS or PEDOT:PSS/PEO solution was then printed onto the treated PDMS substrate using a GIX Microplotter (Sonoplot Inc.) with nozzle openings of 50−400 μm. After printing, the samples were placed on a hot plate and annealed at 120 °C for 15 min. Due to the high boiling point of glycerol, the sample of PEDOT:PSS with 5 wt % glycerol additive was annealed at 150 °C for 60 min. To investigate the printability and optimize the printing results, we have systematically studied the rheological

https://doi.org/10.1021/acsami.1c00537
ACS Appl. Mater. Interfaces 2021, 13, 21693−21702

properties and surface tension of various ink formulations, and the results are shown in Supporting Information Figure S4 and Table S2.

Characterization of the Printed PEDOT:PSS Thin Films. The width (W) and length (L) of the inkjet-printed PEDOT:PSS thin films were measured by an optical microscope (Olympus BX53M). A semiconductor device analyzer (Keysight B1500A) was used to measure the electrical resistance (R) of the printed feature. The sheet resistance (R_s) was calculated with $R_s = R/(L/W)$. The thickness and microstructure of the thin films were measured and captured by an environmental scanning electron microscope (Thermofisher Quattro S ESEM) and an atomic force microscope (Bruker Dimensions ICO AFM). The cyclic stretching test of the thin films was performed on a modified syringe pump with 3D-printed clamps. Eutectic gallium–indium (EGaIn) was placed on both ends of the thin film and connected with copper wires to the semiconductor device analyzer (Keysight B1500A) to acquire the sheet resistance (R_s).

Fabrication and Characterization of the Sensor Patch with ECG and PPG Sensors. The stretchable conductors were prepared using the PEDOT:PSS/PEO solution containing the 50 wt % as-prepared PEO solution (10 mg/mL), 5 wt % ethylene glycol, and 1 wt % Triton-X 100. The solution was then inkjet-printed onto a 0.5 mm thick PDMS substrate pretreated by oxygen plasma (30 W for 15 s) followed by annealing at 120 °C for 15 min. A 3D-printed plastic stencil mask was used for patterning conductive silver epoxy as the binder between stretchable PEDOT:PSS/PEO conductors and other electronic components including light-emitting diode, photodiode, and copper wires. The electrocardiogram was captured by placing three separate PEDOT:PSS/PEO electrodes on the human body (wrist, finger, and thigh) and connected to a commercial heart rate monitor IC (AD8232, SparkFun). The photoplethysmography was achieved by pairing a red light-emitting diode (625 nm, XPEBRD-L1-0000-00501, Cree Inc.) and a photodiode (PDB-C152SMCT-ND, Advanced Photonix). A 5 V reverse bias was applied to the photodiode, and the photocurrent was recorded using a semiconductor device analyzer (Keysight B1500A). The experiment involving a human subject has been performed with the full, informed consent of the volunteer, who is also the first author of the manuscript.

■ ASSOCIATED CONTENT

Supporting Information

The Supporting Information is available free of charge at https://pubs.acs.org/doi/10.1021/acsami.1c00537.

UV–vis spectra of inkjet-printed PEDOT:PSS thin film (Figure S1), electrical characterization of the printed PEDOT:PSS/PEO thin film over time (Figure S2), electrical properties of the PEDOT:PSS/PEO thin film when stretched along the transverse direction (Figure S3), rheological properties of the PEDOT:PSS-based conducting polymer ink (Figure S4), comparison of PEDOT:PSS-based conductor with various kinds of treatment and fabrication methods (Table S1), and summary of ink formulations and measured properties (Table S2) (PDF)

■ AUTHOR INFORMATION

Corresponding Author

Chuan Wang − *Department of Electrical & Systems Engineering and Institute of Materials Science and Engineering, Washington University in St. Louis, St. Louis, Missouri 63130, United States;* orcid.org/0000-0002-5296-0631; Email: chuanwang@wustl.edu

Authors

Li-Wei Lo − *Department of Electrical & Systems Engineering and Institute of Materials Science and Engineering, Washington University in St. Louis, St. Louis, Missouri 63130, United States*

Junyi Zhao − *Department of Electrical & Systems Engineering, Washington University in St. Louis, St. Louis, Missouri 63130, United States*

Haochuan Wan − *Department of Electrical & Systems Engineering, Washington University in St. Louis, St. Louis, Missouri 63130, United States*

Yong Wang − *Department of Electrical & Systems Engineering and Department of Obstetrics & Gynecology, Washington University in St. Louis, St. Louis, Missouri 63130, United States*

Shantanu Chakrabartty − *Department of Electrical & Systems Engineering, Washington University in St. Louis, St. Louis, Missouri 63130, United States*

Complete contact information is available at: https://pubs.acs.org/10.1021/acsami.1c00537

Notes

The authors declare no competing financial interest.

■ ACKNOWLEDGMENTS

This work was supported in whole by the Bill & Melinda Gates Foundation [INV-005417]. The authors acknowledge the Institute of Materials Science and Engineering at Washington University for the use of instruments and staff assistance and Professor Patricia Weisensee's group for help with the ink surface tension measurement.

■ REFERENCES

(1) Bi, C.; Chen, B.; Wei, H.; DeLuca, S.; Huang, J. Efficient Flexible Solar Cell Based on Composition-Tailored Hybrid Perovskite. *Adv. Mater.* **2017**, *29*, 1605900.

(2) Takei, K.; Honda, W.; Harada, S.; Arie, T.; Akita, S. Toward Flexible and Wearable Human-Interactive Health-Monitoring Devices. *Adv. Healthcare Mater.* **2015**, *4*, 487–500.

(3) Khan, Y.; Han, D.; Pierre, A.; Ting, J.; Wang, X.; Lochner, C. M.; Bovo, G.; Yaacobi-Gross, N.; Newsome, C.; Wilson, R.; Arias, A. C. A Flexible Organic Reflectance Oximeter Array. *Proc. Natl. Acad. Sci. U. S. A.* **2018**, *115*, E11015–E11024.

(4) Choi, M.; Park, Y. J.; Sharma, B. K.; Bae, S. R.; Kim, S. Y.; Ahn, J. H. Flexible Active-Matrix Organic Light-Emitting Diode Display Enabled by MoS_2 Thin-Film Transistor. *Sci. Adv.* **2018**, *4*, No. eaas8721.

(5) Gao, W.; Emaminejad, S.; Nyein, H. Y. Y.; Challa, S.; Chen, K.; Peck, A.; Fahad, H. M.; Ota, H.; Shiraki, H.; Kiriya, D.; Lien, D.-H.; Brooks, G. A.; Davis, R. W.; Javey, A. Fully Integrated Wearable Sensor Arrays for Multiplexed in Situ Perspiration Analysis. *Nature* **2016**, *529*, 509–514.

(6) Yu, M.; Wan, H.; Cai, L.; Miao, J.; Zhang, S.; Wang, C. Fully Printed Flexible Dual-Gate Carbon Nanotube Thin-Film Transistors with Tunable Ambipolar Characteristics for Complementary Logic Circuits. *ACS Nano* **2018**, *12*, 11572–11578.

(7) Wan, H.; Cao, Y.; Lo, L.-W.; Zhao, J.; Sepúlveda, N.; Wang, C. Flexible Carbon Nanotube Synaptic Transistor for Neurological Electronic Skin Applications. *ACS Nano* **2020**, *14*, 10402–10412.

(8) Rao, Z.; Ershad, F.; Almasri, A.; Gonzalez, L.; Wu, X.; Yu, C. Soft Electronics for the Skin: From Health Monitors to Human–Machine Interfaces. *Adv. Mater. Technol.* **2020**, *5*, 2000233.

(9) Jeong, Y. R.; Kim, J.; Xie, Z.; Xue, Y.; Won, S. M.; Lee, G.; Jin, S. W.; Hong, S. Y.; Feng, X.; Huang, Y.; Rogers, J. A.; Ha, J. S. A Skin-Attachable, Stretchable Integrated System Based on Liquid GaInSn for Wireless Human Motion Monitoring with Multi-Site Sensing Capabilities. *NPG Asia Mater.* **2017**, *9*, No. e443.

(10) Chortos, A.; Bao, Z. Skin-Inspired Electronic Devices. *Mater. Today* **2014**, *17*, 321−331.
(11) Honda, W.; Harada, S.; Arie, T.; Akita, S.; Takei, K. Wearable, Human-Interactive, Health-Monitoring, Wireless Devices Fabricated by Macroscale Printing Techniques. *Adv. Funct. Mater.* **2014**, *24*, 3299−3304.
(12) Yamamoto, Y.; Yamamoto, D.; Takada, M.; Naito, H.; Arie, T.; Akita, S.; Takei, K. Efficient Skin Temperature Sensor and Stable Gel-Less Sticky ECG Sensor for a Wearable Flexible Healthcare Patch. *Adv. Healthcare Mater.* **2017**, *6*, 1700495.
(13) Zhang, S.; Cai, L.; Li, W.; Miao, J.; Wang, T.; Yeom, J.; Sepúlveda, N.; Wang, C. Fully Printed Silver-Nanoparticle-Based Strain Gauges with Record High Sensitivity. *Adv. Electron. Mater.* **2017**, *3*, 1700067.
(14) Cotur, Y.; Kasimatis, M.; Kaisti, M.; Olenik, S.; Georgiou, C.; Güder, F. Stretchable Composite Acoustic Transducer for Wearable Monitoring of Vital Signs. *Adv. Funct. Mater.* **2020**, *30*, 1910288.
(15) Cai, L.; Zhang, S.; Zhang, Y.; Li, J.; Miao, J.; Wang, Q.; Yu, Z.; Wang, C. Direct Printing for Additive Patterning of Silver Nanowires for Stretchable Sensor and Display Applications. *Adv. Mater. Technol.* **2018**, *3*, 1700232.
(16) Bade, S. G. R.; Shan, X.; Hoang, P. T.; Li, J.; Geske, T.; Cai, L.; Pei, Q.; Wang, C.; Yu, Z. Stretchable Light-Emitting Diodes with Organometal-Halide-Perovskite−Polymer Composite Emitters. *Adv. Mater.* **2017**, *29*, 1607053.
(17) Pu, X.; Liu, M.; Chen, X.; Sun, J.; Du, C.; Zhang, Y.; Zhai, J.; Hu, W.; Wang, Z. L. Ultrastretchable, Transparent Triboelectric Nanogenerator as Electronic Skin for Biomechanical Energy Harvesting and Tactile Sensing. *Sci. Adv.* **2017**, *3*, No. e1700015.
(18) Rogers, J. A.; Someya, T.; Huang, Y. Materials and Mechanics for Stretchable Electronics. *Science* **2010**, *327*, 1603−1607.
(19) Lo, L. W.; Shi, H.; Wan, H.; Xu, Z.; Tan, X.; Wang, C. Inkjet-Printed Soft Resistive Pressure Sensor Patch for Wearable Electronics Applications. *Adv. Mater. Technol.* **2020**, *5*, 1900717.
(20) Shi, H.; Al-Rubaiai, M.; Holbrook, C. M.; Miao, J.; Pinto, T.; Wang, C.; Tan, X. Screen-Printed Soft Capacitive Sensors for Spatial Mapping of Both Positive and Negative Pressures. *Adv. Funct. Mater.* **2019**, *29*, 1809116.
(21) Tang, J.; Guo, H.; Zhao, M.; Yang, J.; Tsoukalas, D.; Zhang, B.; Liu, J.; Xue, C.; Zhang, W. Highly Stretchable Electrodes on Wrinkled Polydimethylsiloxane Substrates. *Sci. Rep.* **2015**, *5*, 16527.
(22) Khang, D. Y.; Rogers, J. A.; Lee, H. H. Mechanical Buckling: Mechanics, Metrology, and Stretchable Electronics. *Adv. Funct. Mater.* **2009**, *19*, 1526−1536.
(23) Sun, Y.; Kumar, V.; Adesida, I.; Rogers, J. A. Buckled and Wavy Ribbons of GaAs for High-Performance Electronics on Elastomeric Substrates. *Adv. Mater.* **2006**, *18*, 2857−2862.
(24) Kim, T.; Park, J.; Sohn, J.; Cho, D.; Jeon, S. Bioinspired, Highly Stretchable, and Conductive Dry Adhesives Based on 1D-2D Hybrid Carbon Nanocomposites for All-in-One ECG Electrodes. *ACS Nano* **2016**, *10*, 4770−4778.
(25) Oh, J. Y.; Jun, G. H.; Jin, S.; Ryu, H. J.; Hong, S. H. Enhanced Electrical Networks of Stretchable Conductors with Small Fraction of Carbon Nanotube/Graphene Hybrid Fillers. *ACS Appl. Mater. Interfaces* **2016**, *8*, 3319−3325.
(26) Larmagnac, A.; Eggenberger, S.; Janossy, H.; Vörös, J. Stretchable Electronics Based on Ag-PDMS Composites. *Sci. Rep.* **2014**, *4*, 7254.
(27) Kim, Y.; Zhu, J.; Yeom, B.; Di Prima, M.; Su, X.; Kim, J. G.; Yoo, S. J.; Uher, C.; Kotov, N. A. Stretchable Nanoparticle Conductors with Self-Organized Conductive Pathways. *Nature* **2013**, *500*, 59−63.
(28) Hu, W.; Niu, X.; Li, L.; Yun, S.; Yu, Z.; Pei, Q. Intrinsically Stretchable Transparent Electrodes Based on Silver-Nanowire-Cross-linked-Polyacrylate Composites. *Nanotechnology* **2012**, *23*, 344002.
(29) Chen, Y.; Carmichael, R. S.; Carmichael, T. B. Patterned, Flexible, and Stretchable Silver Nanowire/Polymer Composite Films As Transparent Conductive Electrodes. *ACS Appl. Mater. Interfaces* **2019**, *11*, 31210−31219.
(30) Tseng, Y.-T.; Lin, Y.-C.; Shih, C.-C.; Hsieh, H.-C.; Lee, W.-Y.; Chiu, Y.-C.; Chen, W.-C. Morphology and Properties of PEDOT:PSS/Soft Polymer Blends through Hydrogen Bonding Interaction and Their Pressure Sensor Application. *J. Mater. Chem. C* **2020**, *8*, 6013−6024.
(31) Dauzon, E.; Lin, Y.; Faber, H.; Yengel, E.; Sallenave, X.; Plesse, C.; Goubard, F.; Amassian, A.; Anthopoulos, T. D. Stretchable and Transparent Conductive PEDOT:PSS-Based Electrodes for Organic Photovoltaics and Strain Sensors Applications. *Adv. Funct. Mater.* **2020**, *30*, 2001251.
(32) Lee, J. H.; Jeong, Y. R.; Lee, G.; Jin, S. W.; Lee, Y. H.; Hong, S. Y.; Park, H.; Kim, J. W.; Lee, S.-S.; Ha, J. S. Highly Conductive, Stretchable, and Transparent PEDOT:PSS Electrodes Fabricated with Triblock Copolymer Additives and Acid Treatment. *ACS Appl. Mater. Interfaces* **2018**, *10*, 28027−28035.
(33) Li, P.; Sun, K.; Ouyang, J. Stretchable and Conductive Polymer Films Prepared by Solution Blending. *ACS Appl. Mater. Interfaces* **2015**, *7*, 18415−18423.
(34) Choong, C.-L.; Shim, M.-B.; Lee, B.-S.; Jeon, S.; Ko, D.-S.; Kang, T.-H.; Bae, J.; Lee, S. H.; Byun, K.-E.; Im, J.; Jeong, Y. J.; Park, C. E.; Park, J.-J.; Chung, U.-I. Highly Stretchable Resistive Pressure Sensors Using a Conductive Elastomeric Composite on a Micropyramid Array. *Adv. Mater.* **2014**, *26*, 3451−3458.
(35) Vosgueritchian, M.; Lipomi, D. J.; Bao, Z. Highly Conductive and Transparent PEDOT:PSS Films with a Fluorosurfactant for Stretchable and Flexible Transparent Electrodes. *Adv. Funct. Mater.* **2012**, *22*, 421−428.
(36) Lipomi, D. J.; Lee, J. A.; Vosgueritchian, M.; Tee, B. C.-K.; Bolander, J. A.; Bao, Z. Electronic Properties of Transparent Conductive Films of PEDOT:PSS On Stretchable Substrates. *Chem. Mater.* **2012**, *24*, 373.
(37) Jung, S.; Sou, A.; Gili, E.; Sirringhaus, H. Inkjet-Printed Resistors with a Wide Resistance Range for Printed Read-Only Memory Applications. *Org. Electron.* **2013**, *14*, 699−702.
(38) Hoath, S. D.; Hsiao, W. K.; Martin, G. D.; Jung, S.; Butler, S. A.; Morrison, N. F.; Harlen, O. G.; Yang, L. S.; Bain, C. D.; Hutchings, I. M. Oscillations of Aqueous PEDOT:PSS Fluid Droplets and the Properties of Complex Fluids in Drop-on-Demand Inkjet Printing. *J. Non-Newtonian Fluid Mech.* **2015**, *223*, 28−36.
(39) Basak, I.; Nowicki, G.; Ruttens, B.; Desta, D.; Prooth, J.; Jose, M.; Nagels, S.; Boyen, H. G.; D'haen, J.; Buntinx, M.; Deferme, W. Inkjet Printing of PEDOT:PSS Based Conductive Patterns for 3D Forming Applications. *Polymer* **2020**, *12*, 2915.
(40) Li, L.; Pan, L.; Ma, Z.; Yan, K.; Cheng, W.; Shi, Y.; Yu, G. All Inkjet-Printed Amperometric Multiplexed Biosensors Based on Nanostructured Conductive Hydrogel Electrodes. *Nano Lett.* **2018**, *18*, 3322−3327.
(41) Huang, T.-T.; Wu, W. Inkjet-Printed Wearable Nanosystems for Self-Powered Technologies. *Adv. Mater. Interfaces* **2020**, *7*, 2000015.
(42) Sico, G.; Montanino, M.; De Girolamo Del Mauro, A.; Minarini, C. Improving the Gravure Printed PEDOT:PSS Electrode by Gravure Printing DMSO Post-Treatment. *J. Mater. Sci.: Mater. Electron.* **2018**, *29*, 11730−11737.
(43) Sico, G.; Montanino, M.; De Girolamo Del Mauro, A.; Imparato, A.; Nobile, G.; Minarini, C. Effects of the Ink Concentration on Multi-Layer Gravure-Printed PEDOT:PSS. *Org. Electron.* **2016**, *28*, 257−262.
(44) Fan, X.; Nie, W.; Tsai, H.; Wang, N.; Huang, H.; Cheng, Y.; Wen, R.; Ma, L.; Yan, F.; Xia, Y. PEDOT:PSS for Flexible and Stretchable Electronics: Modifications, Strategies, and Applications. *Adv. Sci.* **2019**, *6*, 1900813.
(45) Carrasco-Torres, G.; Valdés-Madrigal, M. A.; Vásquez-Garzón, V. R.; Baltiérrez-Hoyos, R.; De la Cruz-Burelo, E.; Román-Doval, R.; Valencia-Lazcano, A. A. Effect of Silk Fibroin on Cell Viability in Electrospun Scaffolds of Polyethylene Oxide. *Polymer* **2019**, *11*, 451.
(46) Vomero, M.; Castagnola, E.; Ciarpella, F.; Maggiolini, E.; Goshi, N.; Zucchini, E.; Carli, S.; Fadiga, L.; Kassegne, S.; Ricci, D. Highly Stable Glassy Carbon Interfaces for Long-Term Neural

https://doi.org/10.1021/acsami.1c00537
ACS Appl. Mater. Interfaces 2021, 13, 21693−21702

Stimulation and Low-Noise Recording of Brain Activity. *Sci. Rep.* **2017**, *7*, 40332.
(47) Jabbar, F.; Soomro, A. M.; Lee, J.-w.; Ali, M.; Kim, Y. S.; Lee, S.-h.; Choi, K. H. Robust Fluidic Biocompatible Strain Sensor Based on PEDOT:PSS/CNT Composite for Human-Wearable and High-End Robotic Applications. *Sens. Mater.* **2020**, *32*, 4077−4093.
(48) Monteiro, A. I.; Kollmetz, T.; Musson, D. S.; McGlashan, S. R.; Malmström, J. Polystyrene-Block-Polyethylene Oxide Thin Films: In Vitro Cytocompatibility and Protein Adsorption Testing. *Biointerphases* **2020**, *15*, No. 011003.
(49) Ouyang, J.; Xu, Q.; Chu, C.-W.; Yang, Y.; Li, G.; Shinar, J. On the Mechanism of Conductivity Enhancement in Poly(3,4-Ethylenedioxythiophene):Poly(Styrene Sulfonate) Film through Solvent Treatment. *Polymer* **2004**, *45*, 8443.
(50) Wijeratne, K.; Ail, U.; Brooke, R.; Vagin, M.; Liu, X.; Fahlman, M.; Crispin, X. Bulk Electronic Transport Impacts on Electron Transfer at Conducting Polymer Electrode−Electrolyte Interfaces. *Proc. Natl. Acad. Sci. U. S. A.* **2018**, *115*, 11899.
(51) Wang, Y.; Song, R.; Li, Y.; Shen, J. Understanding Tapping-Mode Atomic Force Microscopy Data on the Surface of Soft Block Copolymers. *Surf. Sci.* **2003**, *530*, 136−148.
(52) Kayser, L. V.; Lipomi, D. J. Stretchable Conductive Polymers and Composites Based on PEDOT and PEDOT:PSS. *Adv. Mater.* **2019**, *31*, 1806133.
(53) Luo, R.; Li, H.; Du, B.; Zhou, S.; Zhu, Y. A Simple Strategy for High Stretchable, Flexible and Conductive Polymer Films Based on PEDOT:PSS-PDMS Blends. *Org. Electron.* **2020**, *76*, 105451.
(54) Taroni, P. J.; Santagiuliana, G.; Wan, K.; Calado, P.; Qiu, M.; Zhang, H.; Pugno, N. M.; Palma, M.; Stingelin-Stutzman, N.; Heeney, M.; Fenwick, O.; Baxendale, M.; Bilotti, E. Toward Stretchable Self-Powered Sensors Based on the Thermoelectric Response of PEDOT:PSS/Polyurethane Blends. *Adv. Funct. Mater.* **2018**, *28*, 1704285.
(55) Ratna, D.; Divekar, S.; Samui, A. B.; Chakraborty, B. C.; Banthia, A. K. Poly(Ethylene Oxide)/Clay Nanocomposite: Thermo-mechanical Properties and Morphology. *Polymer* **2006**, *47*, 4068−4074.
(56) Wang, T.; Qi, Y.; Xu, J.; Hu, X.; Chen, P. Effects of Poly(Ethylene Glycol) on Electrical Conductivity of Poly(3,4-Ethylenedioxythiophene)-Poly(Styrenesulfonic Acid) Film. *Appl. Surf. Sci.* **2005**, *250*, 188−194.
(57) Yuk, H.; Lu, B.; Zhao, X. Hydrogel Bioelectronics. *Chem. Soc. Rev.* **2019**, *48*, 1642−1667.
(58) Tamura, T.; Maeda, Y.; Sekine, M.; Yoshida, M. Wearable Photoplethysmographic Sensors—Past and Present. *Electrons* **2014**, *3*, 282−302.
(59) Klabunde, R. E. Cardiac Electrophysiology: Normal and Ischemic Ionic Currents and the ECG. *Adv. Physiol. Educ.* **2017**, *41*, 29−37.
(60) Luz, E. J. d. S.; Schwartz, W. R.; Cámara-Chávez, G.; Menotti, D. ECG-Based Heartbeat Classification for Arrhythmia Detection: A Survey. *Comput. Methods Programs Biomed.* **2016**, *127*, 144−164.
(61) Birnbaum, Y.; Drew, B. J. The Electrocardiogram in ST Elevation Acute Myocardial Infarction: Correlation with Coronary Anatomy and Prognosis. *Postgrad. Med. J.* **2003**, *79*, 490−504.

https://doi.org/10.1021/acsami.1c00537
ACS Appl. Mater. Interfaces 2021, 13, 21693−21702